



## Original software publication

## DDRS4PALS: A software for the acquisition and simulation of lifetime spectra using the DRS4 evaluation board



Danny Petschke\*, Torsten E.M. Staab

University Wuerzburg, Department of Chemistry, LCTM Roentgenring 11, D-97070 Wuerzburg, Germany

## ARTICLE INFO

## Article history:

Received 6 March 2019

Received in revised form 13 June 2019

Accepted 13 June 2019

## Keywords:

Lifetime spectroscopy

Positron annihilation spectroscopy

Simulation

Time resolved measurements

## ABSTRACT

Lifetime techniques are applied to diverse fields of study including materials sciences, semiconductor physics, biology, molecular biophysics and photochemistry.

Here we present *DDRS4PALS*, a software for the acquisition and simulation of lifetime spectra using the DRS4 evaluation board (Paul Scherrer Institute, Switzerland) for time resolved measurements and digitization of detector output pulses. Artifact afflicted pulses can be corrected or rejected prior to the lifetime calculation to provide the generation of high-quality lifetime spectra, which are crucial for a profound analysis, i.e. the decomposition of the *true* information. Moreover, the pulses can be streamed on an (external) hard drive during the measurement and subsequently downloaded in the offline mode without being connected to the hardware. This allows the generation of various lifetime spectra at different configurations from one single measurement and, hence, a meaningful comparison in terms of analyzability and quality. Parallel processing and an integrated JavaScript based language provide convenient options to accelerate and automate time consuming processes such as lifetime spectra simulations.

© 2019 The Authors. Published by Elsevier B.V. This is an open access article under the CC BY license (<http://creativecommons.org/licenses/by/4.0/>).

## Code metadata

Current code version	v1.08
Permanent link to code/repository used of this code version	<a href="https://github.com/ElsevierSoftwareX/SOFTX_2019_65">https://github.com/ElsevierSoftwareX/SOFTX_2019_65</a>
Legal Code License	GNU General Public License v3
Code versioning system used	github
Software code languages, tools, and services used	C/C++, Qt framework <b>third party libraries:</b> ALGLIB, Tino Kluge: a cubic spline interpolation library, Sergejus Zabinski: fast median filtering, MPFIT: A MINPACK-1 least squares fitting library in C, libusb-1.0 package: USB device access, DRS4 eval board API (Paul Scherrer Institute, Switzerland), DLTPulseGenerator: a library for the simulation of lifetime spectra based on detector-output pulses
Compilation requirements, operating environments & dependencies	<b>OS:</b> Microsoft Windows <b>compilation requirements:</b> <b>Qt-framework</b> (at least v5.x), MS Visual Studio Compiler (at least) 2013 <b>hardware required for the acquisition mode:</b> DRS4 evaluation board by Paul Scherrer Institute (PSI, Switzerland): <a href="https://www.psi.ch/en/drs/evaluation-board">https://www.psi.ch/en/drs/evaluation-board</a>

\* Corresponding author.

E-mail addresses: [danny.petschke@uni-wuerzburg.de](mailto:danny.petschke@uni-wuerzburg.de) (D. Petschke), [torsten.staab@uni-wuerzburg.de](mailto:torsten.staab@uni-wuerzburg.de) (T.E.M. Staab).

If available Link to developer documentation/manual

a **readme.md** file can be found on **github**:  
<https://github.com/dpscience/DDRS4PALS/blob/master/README.md>  
[danny.petschke@uni-wuerzburg.de](mailto:danny.petschke@uni-wuerzburg.de)

Support email for questions

## 1. Introduction and significance

Over the last decades, lifetime-based spectroscopy techniques have become established methods in the fields of life and materials sciences.

In biomedical studies, fluorescence lifetime spectroscopy (FLS) and imaging techniques, such as fluorescence lifetime correlation spectroscopy (FLCS) or fluorescence lifetime imaging microscopy (FLIM), are powerful tools to elucidate the intra and intermolecular dynamics of protein activation, interaction and diffusion [1,2]. The fluorescence lifetime is a measure of time a fluorophore spends in the excited state before relaxation into the ground state by emitting a photon.

In positron annihilation lifetime spectroscopy (PALS) the lifetime of an antielectron (positron) is directly measured through gamma rays accompanying its creation (e.g. from a  $\beta^+$  decay at 22-Na) and annihilation with an electron. This method provides a powerful technique for non-destructive microstructure investigations in a broad range of material classes from metals [3–8] and semiconductors [9,10] to polymers [11,12] and porous glasses [13,14]. The characteristic lifetimes are highly sensitive to the kind and size of atomic like defects (e.g. vacancies or nanometer-sized pores) ranging from approximately hundred picoseconds to a maximum of 142 nanoseconds.

Nowadays, a classical lifetime spectroscopy setup (FLS, PALS) consists of photomultipliers or photodiodes (e.g. APD), which serve for the detection of single photons representing the start and stop events, and a digitizer for the time resolved acquisition and digitization of the corresponding output pulses.

However, in the positron community, the transfer from conventional analog NIM (nuclear instrument modules) electronics to digital acquisition systems, such as the here employed DRS4 evaluation board (hereafter called *DRS4-EB*), is not consequently implemented regardless to its great benefits in terms of spectra quality and analyzability as first demonstrated in the 2000th [15–19]. Moreover, the advantages of using digital setups for the method of PALS includes configurations and adjustments easily managed by software:

- corrections and filters can be applied on the acquired (and digitized) detector output pulses prior to the generation of the lifetime spectrum → exclusion of odd or false-true events from the lifetime spectrum,
- configurations can be (re-)stored, which allows setup and data reproducibility,
- time consuming adjustment processes on the analog NIM electronics are completely dispensable.

The here presented software *DDRS4PALS*<sup>1</sup> (v1.08 [20]) allows to take advantage of the above stated benefits by using digital setups based on the *DRS4-EB* provided by the Paul Scherrer Institute (PSI, Switzerland) [21–23]. The first PALS application employing the *DRS4-EB* in combination with a self-written software tool called *QtPALS* was first shown by Petriska et al. in 2014 [24]. To the best of the authors knowledge, the *DRS4-EB* has not yet been applied to fluorescence lifetime spectroscopy setups. However, at

this stage *DDRS4PALS* can be easily applied for FLS as conventional setups use photomultipliers and/or photodiodes for the detection of the photons similar to the technique of PALS.

This publication of *DDRS4PALS* should bring wider adoption to the positron community of using digital setups for the method of PALS as this software provides a user-friendly graphical interface (GUI), which allows to easily manage all setup configurations and settings related to the acquisition process. Therefore, we give a detailed description of the internal software functionality and the applied algorithms to provide full transparency regarding the pulse acquisition and subsequent spectra generation.

## 2. Software features & functionalities and requirements on the hardware

### • Requirements on the hardware

*DDRS4PALS* is written in C++ using the *Qt-framework* [25]. Basically, this software is designed for the acquisition (and simulation) of lifetime spectra using photomultipliers or photodiodes arranged in a two-detector (2-D) setup for the detection of the start and stop photons, and the *DRS4-EB* for the time resolved measurement and subsequent digitization of the respective analog output pulses.<sup>2</sup> The time differences, i.e. the lifetimes, which form the resulting lifetime spectra, are calculated from a pair of output pulses that coincide within a defined time frame (called *sweep* hereafter). The accurate timing points of the output pulses are determined on the rising edge by applying the constant fraction (CF) principle, which is preferably used on signal shapes having a constant rise time at varying pulse heights (see 2.1). Furthermore, an overall readout range of  $\pm 500$  mV on the analog inputs (Chn1 & Chn2) of the *DRS4-EB* is required (see footnote 2).

### • Software modii: acquisition (online) & simulation (offline) mode

As illustrated in Fig. 1, *DDRS4PALS* provides two modii: the (1) *acquisition* and the (2) *simulation & pulse analysis mode* (hereafter called *simulation mode*). In the *acquisition mode*, a connection to the *DRS4-EB* is required (online). Here, the lifetime spectra are either directly generated from the acquired output pulses using a certain software configuration file (Table 1) or, instead, the raw output pulses are streamed (uploaded) on an external hard drive without considering any corrections or filters (see 2.2). Subsequently, the recorded output pulses can be downloaded in the *simulation mode* (offline) as if they were acquired in the *acquisition mode*. This allows the generation of various lifetime spectra at any time by applying different software configurations, i.e. settings on a single measurement and, moreover, a meaningful comparison in terms of analyzability and quality is provided (see 3). Once a reasonable software configuration was determined in the *simulation mode*, it can be used for the subsequent measurements in the *acquisition mode*. Furthermore, this mode provides the simulation of lifetime spectra based on realistically modeled detector output pulses by using our previously released library *DLTPulseGenerator* [27–30]. A *xml file* serves as

<sup>1</sup> Explanation of abbreviation *DDRS4PALS*: The first 'D' stands for the initials of the first authors forename, *DRS4* for the *DRS4-EB* and *PALS* for positron annihilation lifetime spectroscopy as this software was generally developed on this technique.

<sup>2</sup> For further details regarding the setup requirements in combination with *DDRS4PALS* for studies which use the method of positron annihilation lifetime spectroscopy (PALS), we refer to our recent publication [26].

**Table 1**  
DDRS4PALS file formats.

File description	File extension
Software configuration	*.drs4LTSettings
Output pulse pair stream	*.drs4DataStream
Simulation input file ( <i>DLTPulseGenerator</i> library)	*.drs4SimulationInputFile
Script file	*.drs4Script

simulation input file (Table 1), where each *tag* and corresponding *element* refers to the name and physical meaning of the parameters as described in the related publications (e.g. `<rise-time-in-ns>5</rise-time-in-ns>` sets the rise time of the output pulse to five nanoseconds).

DDRS4PALS has implemented the *DRS4 API* provided by the Paul-Scherrer Institute (PSI, Switzerland) for accessing the functionality of the *DRS4-EB* [31]. Thus, for further information on the hardware-based configurations, such as the trigger functionality (logic, level, delay) or the sampling frequency (sweep), we refer to the manual of the *DRS4-EB* [22,23]. Note, even though these parameters are stored in the software configuration file (Table 1), they cannot be adjusted afterwards in the *simulation mode*.

The following sections give an insight to the main functionalities of the most relevant features provided by DDRS4PALS. However, several additional features, whose detailed description is not part of this publication, are available:

- ASCII export of the acquired output pulse pairs,
- ASCII export of output pulse pairs, which generate a certain part (lifetime region) in the lifetime spectrum,
- pulse height spectrum (PHS) for energy discrimination of the detected photons: a window describing a defined energy region can be assigned to distinguish the detected output-pulse as being a start or stop event,
- region-of-interest (ROI) within the sweep: sampling points outside this ROI are not considered for the pulse analysis and lifetime calculation,
- online approximation of the instrumental response (IRF) by fitting a single Gaussian distribution function on the left side of the lifetime spectrum,
- persistence plot of the output pulse pairs, whose time differences (lifetimes) are part of the resulting lifetime spectrum,
- *DRS4-EB* temperature control/logging,
- inline calculator

A description and example for the process automation using the integrated scripting functionality can be found in the supplementary (Appendix A).

### 2.1. Constant fraction (CF) principle for accurate timing determination

As shown in Fig. 2, the sampling points on the rising edge (red points) are spline interpolated (blue curve) prior to the determination of the exact timing point by applying the CF principle. Therefore, DDRS4PALS allows to select one of five interpolation types: (1) *linear*, (2) *cubic*, (3) *Akima*, (4) *Cutmull-Rom* and (5) *monotone*. The algorithms of the non-linear interpolation types (2–5) are provided using the *ALGLIB* library [32] internally.

The voltage of a given CF level (e.g. 30% in Fig. 2) is calculated from the pulse height (amplitude) with respect to the zero baseline (see 2.2.1). In case of a linear interpolation (1), the timing point  $t_{CF}$  is directly determined by a straight line obtained by the upper  $t_{i+1}$  and lower  $t_i$  adjacent sampling points (Fig. 2). However, in case of a non-linear interpolation (2–5),  $N$  equidistantly arranged intermediate steps (see Fig. 2a, combo box: ‘Number of Render Points’) are inserted on the time axis in

between the upper ( $t_{i+1}$ ) and lower ( $t_i$ ) sampling points (Fig. 2c). This allows to vary the approximation level, i.e. the render depth of the spline curvature and, moreover, to adjust the precision of the accurate timing point in between two neighboring sampling points.

If the rising edge consists of enough sampling points to clearly represent the true output pulse shape, as shown in the case in Fig. 2a (1024 sampling points/cells at 5.12 GHz), a linear interpolation (1) is almost sufficient. However, the non-linear interpolations (2–5) should be applied in the case of slow sampling speeds (e.g. 1024 sampling points/cells at 1–2 GHz) in combination with output pulses having very short rise times (1–5 ns).

### 2.2. Corrections and filters on the acquired detector output pulses

To assure the generation of high-quality lifetime spectra, DDRS4PALS provides several corrections and filters, which can be applied to reject artifact afflicted output pulses or multiple occurrences of output pulses within the readout range (sweep) prior to the lifetime calculation. Two general types of filters are provided: (1) *intrinsic* filters, which cause modifications on the original waveform (see 2.2.1 and 2.2.2) and (2) *external* filters, which are based on specific properties of the waveform such as its area (see 2.2.3) or shape (see 2.2.4). As soon as an *intrinsic* type filter is activated, the *external* filters are based on the properties of the modified waveforms. Multiple *external* filters applied behave in *OR logic*, meaning that the output pulses are already rejected, if only one of the filters is valid (e.g. `area == true OR shape == true`).

#### 2.2.1. Correction of the baseline-offset jitter and baseline filter

By activating the *baseline correction*, the offset-jitter is corrected/shifted to one set baseline value (see Fig. 3a, combo-box: ‘Baseline’), e.g. the zero baseline (0 mV). The offset value is calculated by averaging a defined cell region (sampling points) fixed within the sweep (see Fig. 3a, combo-boxes: ‘Start-Cell’ and ‘Cell-Region’). To assure a constantly stable timing determination, this correction is mandatory since the CF level is always calculated with respect to the zero baseline (see 2.1). Additionally, the acquired output pulses can be filtered regarding the jitter magnitude, i.e. the deviation between the calculated and the set baseline value (see Fig. 3a, group-box: ‘Baseline Filter’). Thus, output pulses having offset values exceeding the maximum allowed deviation relative to the set baseline value are discarded (see Fig. 3a, blue shaded box). The value for the max. deviation is given in percentage [%] of the absolute value of the overall readout range ( $\pm 500$  mV).

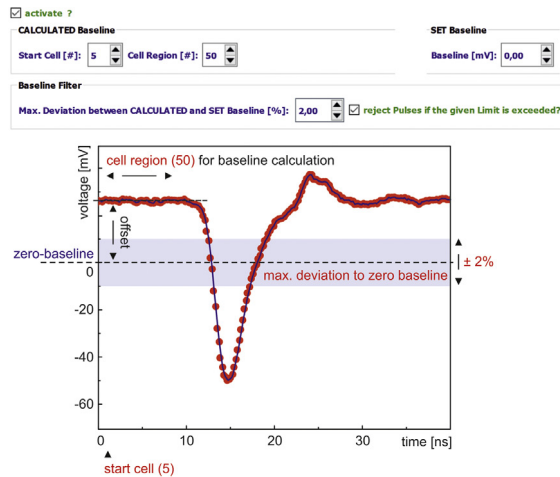
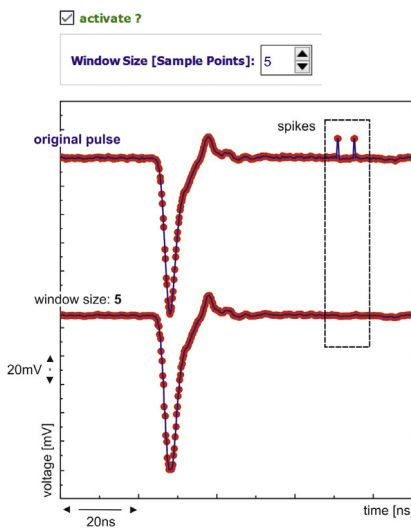
#### 2.2.2. Removal of spike-like artifacts: median filter

As shown in Fig. 3b, spike-like artifacts, which originate from USB cross talks, may occur frequently in the acquired waveforms (Fig. 6a) [22,23]. As those spikes might cause an incorrect timing determination (see 2.1), especially when occurring in the rising edge region, they should be clearly eliminated by applying the median filter. This filter replaces the sampling points by its calculated median value within the defined window size (see Fig. 3b, combo-box: ‘Window-Size’). Obviously, a window size of five sampling points is sufficient to remove all occurring spikes without significantly modifying the waveform, as applied in Fig. 3b.

Note, the window size should be an odd number as the median can be then simply defined by its middle value of the sorted entries, whereas an even number could lead to more than one possible median value.

We used the fast algorithm of the *1D median filter* by Sergejus Zabinski [33].



**(a) baseline correction/filter****(b) median filter**

**Fig. 3.** Intrinsic filters: (a) The baseline offset (-jitter) of the output pulses can be corrected to one set baseline value, e.g. the zero baseline (0 mV). By activating the baseline filter, output pulses having offsets exceeding a max. allowed deviation from the set baseline value (given in % of 500 mV) are rejected. (b) A median filter can be applied to eliminate spike-like artifacts in the waveform data originating from USB cross talks, where the window size represents the number of sampling points used to determine the median.

on the horizontal axis for visualization, an additional scaling factor  $f$  indicated as 'Normalization' factor need to be adjusted. Its relationship is given by

$$A_{\text{ratio}} = \frac{A_{\text{pulse}}}{f A_{\text{ROI}}}, \quad (1)$$

where the input of the scaling factor ( $f$ ) is expected in percentage units [%]. Finally, the area ratios ( $A_{\text{ratio}}$ ) are discretized into a given number of bins defined in the combo-box 'Area-Binning Cnt.' (Fig. 4a, bottom).

**2.2.4. Pulse shape filter**

By activating the pulse shape filter, output pulses, which deviate significantly from an average overall pulse shape can be excluded from the lifetime calculation. The average pulse shape (Fig. 4b, red colored pulse) is calculated from a defined number of recorded output pulses normalized by their amplitude and

then shifted relatively to each other that the timing point at the maximum amplitude represents zero (0 ns) on the time scale. The upper and lower bounding, represented by a fraction of the standard deviation (see Fig. 4b, group-boxes: 'Upper Level (UL)' and 'Lower Level (LL)'), are defined by two pulse-like hull curves (Fig. 4b, blue colored pulses) enclosing the average pulse shape. Therefore, output pulses are rejected if at least one sampling point occurs outside the defined pulse shape bounding within the defined region-of-interest (Fig. 4b, group-box: 'Filter ROI'). Optionally, a record scheme can be applied to consider output pulses only in a defined pulse height region for recording and subsequent calculation of the average pulse shape (Fig. 4b, combo-box: 'record scheme').

**2.3. Parallel computing: multicore threading**

DDRS4PALS provides parallel computing to accelerate pulse analysis and subsequent lifetime calculation by a factor of available CPU cores. This feature is of great advantage in the *simulation mode*, whereas in the *acquisition mode* it provides no additional benefit, since the lifetime efficiency is limited by the USB2.0 transfer rate of the DRS4-EB. As illustrated in Fig. 5, a defined chunk of output pulse pairs is assigned to an idle CPU core for the pulse analysis where, meanwhile, another chunk is acquired and assigned to the next available idle CPU core. Once the analysis is finished on the CPU cores, each generated lifetime spectrum is merged into the resulting lifetime spectrum, which is visible for the user. To take advantage of multicore threading, the chunk size must be adjusted in the way that the ratio is well balanced between the time, which is needed for the CPU core assignment, and the time, which is needed to run the calculation.

The multicore threading functionality in DDRS4PALS is provided by the *QtConcurrent* module [34], which is part of the *Qt framework* [25].

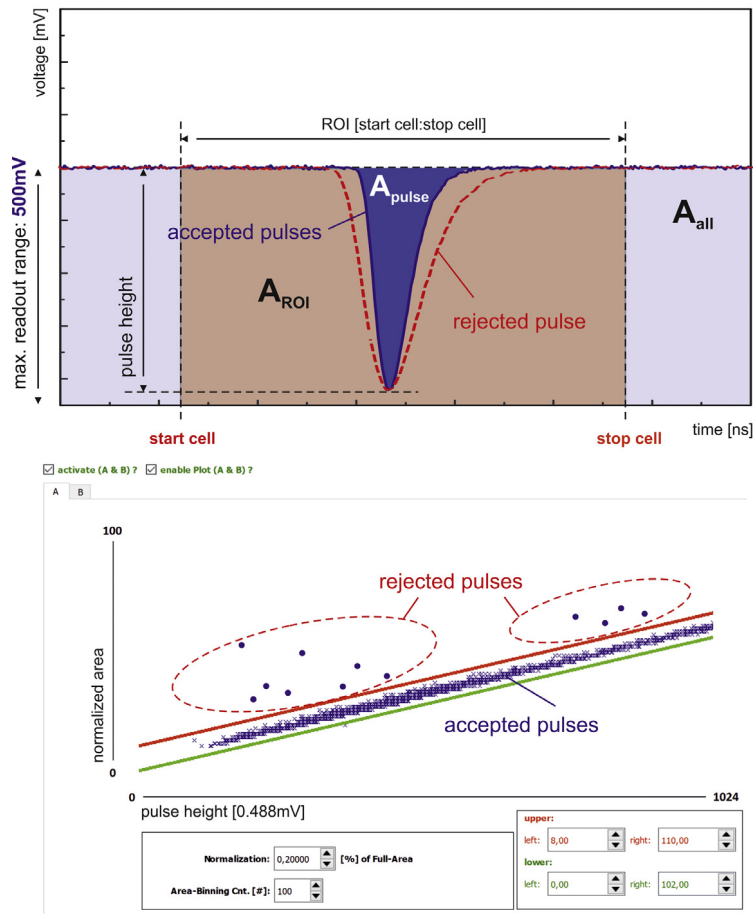
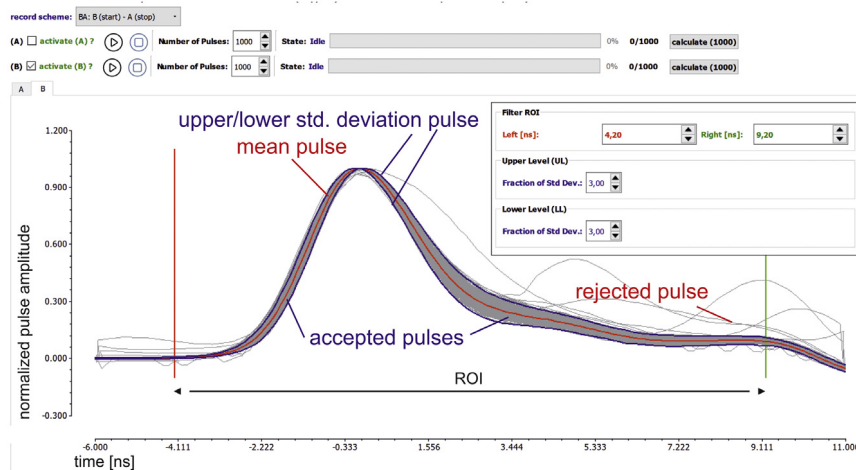
**3. Illustrative example – positron annihilation lifetime spectroscopy (PALS) on pure iron (5N)**

To verify the validity and functionality of DDRS4PALS, two PALS spectra (three million counts) at different software configurations (with and without filters/corrections applied, see Fig. 6), were generated from one single measurement (stream on external hard drive) obtained on pure iron ( $\alpha$ -Fe-5N) by employing the identical setup as detailed described in [26].  $^{22}\text{Na}$  with an activity of 25  $\mu\text{Ci}$  sealed in Kapton foil served as a positron source.

As illustrated in Fig. 6a and b, one can clearly see that by comparing the normalized output pulses (top) and corresponding lifetime spectra (bottom) of both applied software configurations, a correction of the baseline as well as the elimination (or correction) of artifact afflicted output pulses is crucial. This significantly improves the lifetime spectra quality and, finally, its analyzability in terms of decomposing the *true* information, i.e. the characteristic lifetimes  $\tau$  and its contributions  $I$  (see Table 2), as already shown elsewhere by Běčvář [36] and Běčvář et al. [37].

Basically, the shape of the lifetime spectrum is mathematically described by a convolution of the instrumental response (IRF) and a sum of exponential decay functions carrying the relevant information.<sup>3</sup> Hence, additional artifacts in the lifetime spectrum such as indicated on the left side (Fig. 6a, black dashed rectangle) might be as well incorporated in the right-side region, even though they are not directly visible as they appear blurred with the underlying exponential decays. Depending on

<sup>3</sup> For further details regarding the underlying mathematical models, we refer to the publications of the *DLTPulseGenerator* library [27–30] and references given there.

**(a) pulse area filter****(b) pulse shape filter**

**Fig. 4.** External filters: (a) By applying the pulse area filter, pile-up events can be detected. Output pulses with areas outside the defined bounding box adjusted by two straight lines (red and green) are rejected. (b) Output pulses, whose shape deviates significantly from an average pulse shape (red curve), determined from a defined set of recorded output pulses, are rejected. A defined fraction of the determined standard deviation (blue curves) represents the upper and lower bounding within the sampling points of the output pulses are accepted.

the degree/shape of these artifacts and the composition of the lifetime spectrum, this may cause significant deviations in the retrieved information ( $\tau$ , I) with respect to the *true* values, especially when existent in lifetime spectra consisting of relatively

short characteristic lifetimes below (or close to) the FWHM of the Gaussian approximated IRF and/or having multiple components with characteristic lifetimes hardly distinguishable from each other.

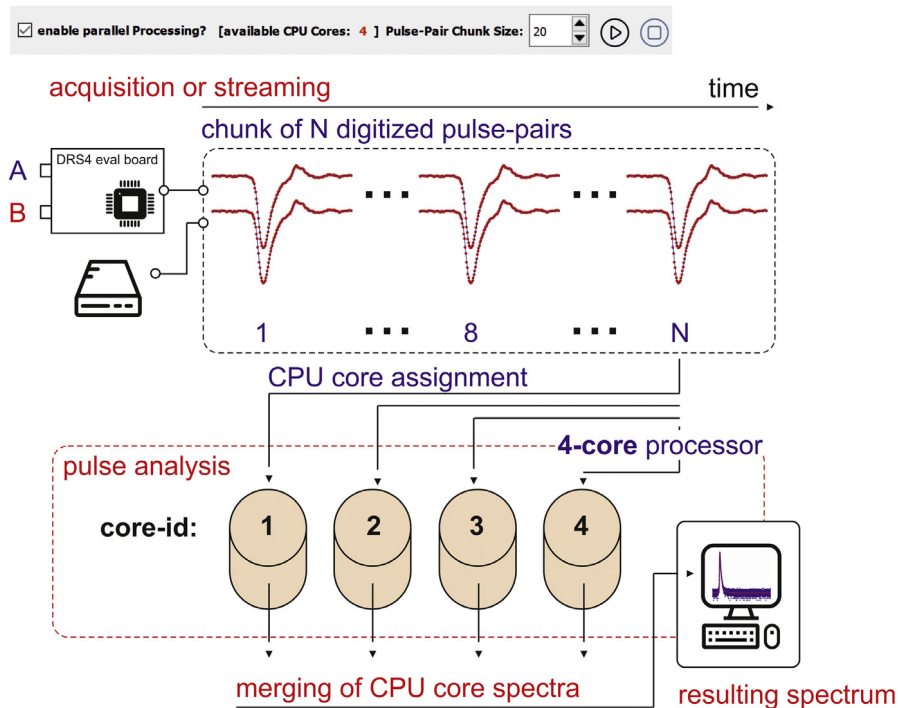


**Fig. 5.** Basic workflow of the parallel computing option: Computationally expensive processes such as pulse analysis and subsequent lifetime spectra generation can be parallelized by the number of available CPU cores (here 4). A defined number of output pulse pairs is assigned to the available number of CPU cores (N), which calculate N lifetime spectra in parallel. Subsequently, the generated lifetime spectra are merged into the resulting lifetime spectrum visible for the user.

For the spectra analysis of high-purity, well annealed metals, three characteristic lifetimes ( $\tau$ ), originating from

- the bulk material (in this case  $\alpha$ -Fe-5N),
- the 22-Na salt and the Kapton foil in combination,
- and the formed ortho-positronium (*o*-Ps)

are expected to be retrieved from the obtained lifetime spectra (see Table 2).

By comparing Fig. 6a and b, the application of corrections and filters on the detector output-pulses eliminates the left-sided artifacts from the lifetime spectrum as can be clearly observed from the disappeared deviations in the residual plot (see Fig. 6 bottom, black dashed rectangle), even though the differences in the goodness-of-fit ( $\chi^2$ ) indicate no significance. Depending on the hardware site setup configurations and used electronic components, those artifacts can appear more pronounced (especially on the left side) as well-known from lifetime spectra acquired with conventional setups consisting of analog NIM electronics only.

Moreover, a considerable improvement of approximately 22% can be noticed in the peak-to-background ratio (Table 2). This clearly increases the feasibility of a more accurate and stable lifetime spectra decomposition, particularly for low-contributed longer characteristic lifetimes, i.e. those of the positronium ( $\tau_3/I_3$ ). Hence, the more accurate extraction of the longest component ( $I_3/\tau_3$ ) leads to a modification of the IRF's effective FWHM affecting the bulk ( $\alpha$ -Fe) and positron source (22-Na) components. Due to this, a significant shift can be noticed in the contributions of the bulk ( $I_1$ ) and positron source ( $I_2$ ) components at the expense of each other. Concerning the characteristic lifetime of the bulk component ( $\tau_1$ ), we are not able to state whether the shift tends to more accurate values, since theoretical calculations show that the characteristic lifetime of iron ( $\alpha$ -Fe) ranges from 101 to 113 ps depending on the applied computational method [38,39]. Moreover, both values lie nearly within its statistical uncertainties.

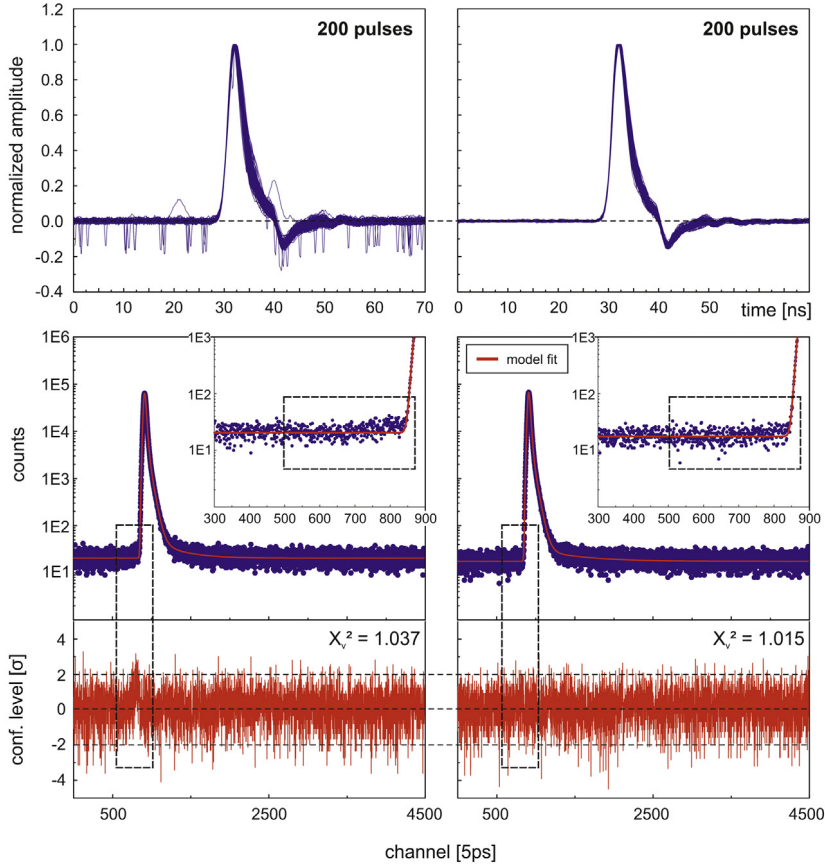
The nomenclature of describing influences on the spectra shape as being *artifact* or *background* can be generally differentiated by its origin: The *background* appears constantly distributed over the time domain of the lifetime spectrum, since it is statistically generated by uncorrelated events originating from falsely assigned start and stop events mainly caused by: (1) Compton scattering in the scintillation materials and (2) pile-up events, meaning that more than one output pulse occurs in the read-out range (sweep) of the corresponding detected photon. On the contrary, *artifacts* are rather of systematic nature and can result from misinterpreted pulses, for instance, due to a wrong determination of the exact timing point caused by artifacts in the detector output-pulses (cf. Fig. 6a, top).

Increasing the activity of the positron sources clearly leads to a rise in the detection efficiency and, thus, to a reduction in the time needed for the generation of the lifetime spectrum (e.g. time-critical measurements). However, the higher activity causes a natural drop in the peak-to-background ratio, since the probability of detecting uncorrelated events significantly rises. Hence, the application of filters, especially the area filter (see 2.2.3) becomes crucial to reduce the background contribution of uncorrelated events stemming from pile-up events, whereas the background contribution resulting from uncorrelated events due to Compton scattering in the scintillation material remains constant as it cannot be suppressed by software-based filters.

#### 4. Impact and conclusion

As reviewed in detail by Istratov & Vyvenko [40], the decomposition of multi-exponential decays and, therefore, that of lifetime spectra is well known to be inherently ill-conditioned [41]. The essential difficulties in the solution of this problem are due to:

- incompleteness:** the acquired data are only given partially and, thus, approximate the lifetime spectrum over a finite range in the time domain,

(a) without filter/corrections applied (b) with filter/corrections applied

**Fig. 6.** PALS on pure iron ( $\alpha$ -Fe-5N): (bottom) Two lifetime spectra (three million counts) generated from one single measurement (stream on external hard drive) and (top) a corresponding set of 200 normalized output pulses (a) without and (b) with baseline correction (2.2.1), median (2.2.2), area (2.2.3) and shape (2.2.4) filters applied. The red line indicates the model fit with the parameters as given in Table 2 accomplished using DQuickLTFit v4.0 [35].

**Table 2**

Results of the PALS spectra obtained from one single measurement on pure iron ( $\alpha$ -Fe-5N) without and with corrections and filters applied (see Fig. 6).  $^{22}\text{Na}$  sealed in Kapton foil served as the positron source ( $\tau_2/I_2$ ). The longest components  $\tau_3$  ( $I_3$ ) results from the lifetime of positrons, which form hydrogen-like atoms (ortho-positronium) in between the source covering foil and the source ( $^{22}\text{Na}$ ) and in between the source covering foil and the sample. The analysis was accomplished using DQuickLTFit v4.0 [34] with no restrictions on the fit parameters, i.e. fixed values. The instrumental response (IRF) is approximated by a sum of two Gaussian distribution functions (see footnote 3).

	<u>Without</u> filters/corrections applied	<u>With</u> filters/corrections applied
$\tau_1$ : $\alpha$ -Fe	<b>104.46</b> (1.27) ps	<b>108.50</b> (1.06) ps
$I_1$ : $\alpha$ -Fe	81.4 (0.4) %	83.1 (0.4) %
$\tau_2$ : source ( $^{22}\text{Na}$ )	353.76 (3.93) ps	362.80 (3.27) ps
$I_2$ : source ( $^{22}\text{Na}$ )	18.11 (0.06) %	16.63 (0.05) %
$\tau_3$ : positronium	1831 (126) ps	2751 (217) ps
$I_3$ : positronium	0.481 (0.005) %	0.301 (0.005) %
$\text{FWHM}_{\text{eff}}$	<b>241.60</b> (2.58) ps	<b>235.39</b> (2.32) ps
peak-to-background ratio	<b>3006</b>	<b>3667</b>
$\chi^2_{\nu}$	<b>1.037</b>	<b>1.015</b>

(ii) **noise**: the acquired data are contaminated by noise and, thus, are not known accurately.

This difficulty even remains existent for synthetically generated lifetime spectra (e.g. see [42]). Therefore, the acquisition of high-quality non-artifact afflicted lifetime spectra must be assured for a quantitative analysis. This can be realized using the here presented software tool *DDRS4PALS*.

*DDRS4PALS* provides the generation of lifetime spectra using the *DRS4-EB* for the time resolved acquisition and subsequent digitization of the detector output pulses. Various filters and

corrections such as the baseline correction, median filter, pulse area or shape filter can be applied on the output pulses prior to the lifetime calculation. This is crucial for the generation of high-quality lifetime spectra and, hence, for its *true* decomposition as it eliminates artifacts present in the lifetime spectrum and, farther, provides a significant improvement in the peak-to-background ratio. We have demonstrated this by employing PALS on pure iron (see 3). The raw output pulses can be streamed on an external hard drive during the acquisition process (online mode) and subsequently downloaded for the lifetime spectra generation in



the offline mode. This allows the generation of various lifetime spectra for different software configurations, i.e. settings on one single measurement and, therefore, a meaningful comparison among each other in terms of analyzability and quality.

Moreover, *DDRS4PALS* has integrated the *DLTPulseGenerator* library, which provides the simulation of realistic lifetime spectra based on detector output pulses by considering the most relevant hardware influences [27–30]. Therefore, it can be used for simulation purposes only, i.e. without being connected to the *DRS4-EB*.

## Acknowledgments

This publication was funded by the German Research Foundation (DFG) and the University of Wuerzburg (Germany) in the funding program Open Access Publishing.

We thank Ricardo Helm from Universität der Bundeswehr (Munich, Germany) for extensively testing *DDRS4PALS* and Hannah Heil from Rudolf Virchow Center of Julius-Maximilians University (Würzburg, Germany) for advice regarding fluorescence spectroscopy techniques. We also say thanks to Jakub Cizek from Charles University (Prague, Czech Republic) and Martin Petriska from Slovak University of Technology (Bratislava, Slovakia) for fruitful discussions during the 18th International Conference on Positron Annihilation (ICPA-18) held in Orlando (2018).

## Declaration of competing interest

The authors declare that they have no known competing financial interests or personal relationships that could have appeared to influence the work reported in this paper.

## Appendix A. Supplementary data

Supplementary material related to this article can be found online at <https://doi.org/10.1016/j.softx.2019.100261>.

## References

- [1] Festy F, Ameer-Beg SM, Ng T, Suhling K, Spagnuolo C, Martinez OE, et al. Imaging proteins in vivo using fluorescence lifetime microscopy. *Mol Biosyst* 2007;3:381. <http://dx.doi.org/10.1039/b617204k>.
- [2] Elson EL. Fluorescence correlation spectroscopy: Past, present, future. *Biophys J* 2011;101:2855–70. <http://dx.doi.org/10.1016/j.bpj.2011.11.012>.
- [3] Connors DC, West RN. Positron annihilation and defects in metals. *Phys Lett A* 1969;30:24–5. [http://dx.doi.org/10.1016/0375-9601\(69\)90018-8](http://dx.doi.org/10.1016/0375-9601(69)90018-8).
- [4] Hautojärvi P, Tamminen A, Jauho P. Trapping of positrons by dislocations in aluminum. *Phys Rev Lett* 1970;24:459–61. <http://dx.doi.org/10.1103/PhysRevLett.24.459>.
- [5] Crisp VHC, Lock DG, West RN. An investigation of positron trapping in indium. *J Phys F: Met Phys* 1974;4:830–8. <http://dx.doi.org/10.1088/0305-4608/4/6/011>.
- [6] Seeger A. Investigation of point defects in equilibrium concentrations with particular reference to positron annihilation techniques. *J Phys F: Met Phys* 1973;3:248–94. <http://dx.doi.org/10.1088/0305-4608/3/2/003>.
- [7] Seeger A. The study of defects in crystals by positron annihilation. *Appl Phys* 1974;4:183–99. <http://dx.doi.org/10.1007/BF00884229>.
- [8] Seeger A. The temperature dependence of the diffusion coefficient and of the trapping rate of positrons in metals. *Appl Phys* 1975;7:257–63. <http://dx.doi.org/10.1007/BF00900321>.
- [9] Saarinen K, Hautojärvi P, Corbel C. Positron annihilation spectroscopy of defects in semiconductors. In: Identif. defects semicond. Elsevier Ltd.; 1998, p. 209–85. [http://dx.doi.org/10.1016/S0080-8784\(08\)63057-4](http://dx.doi.org/10.1016/S0080-8784(08)63057-4).
- [10] Krause-Rehberg R, Leipner HS. *Positron annihilation in semiconductors: Defect studies*. Berlin: Springer; 1999.
- [11] Dlubek G, Kilburn D, Bondarenko V, Pionteck J, Krause-Rehberg R, Alam MA. Positron annihilation: A unique method for studying polymers. *Macromolecular* 2004;210:1–11.
- [12] Harms S, Rätzke K, Faupel F, Schneider GJ, Willner L, Richter D. Free volume of interphases in model nanocomposites studied by positron annihilation lifetime spectroscopy. *Macromolecules* 2010;43:10505–11. <http://dx.doi.org/10.1021/ja1022692>.
- [13] Zaleski R. Ortho-positronium localization in pores of vycor glass at low temperature. *J Phys: Conf Ser* 2013;443: 012062. <http://dx.doi.org/10.1088/1742-6596/443/1/012062>.
- [14] Thränert S, Enke D, Dlubek G, Krause-Rehberg R. Positron lifetime spectroscopy on controlled pore glass porosimetry and pore size distribution. *Mater Sci Forum* 2009;607:169–72. <http://dx.doi.org/10.4028/www.scientific.net/MSF.607.169>.
- [15] Bečvář F, Čížek J, Procházka I, Janotová J. The asset of ultra-fast digitizers for positron-lifetime spectroscopy. *Nucl Instrum Methods Phys Res A* 2005;539:372–85. <http://dx.doi.org/10.1016/j.nima.2004.09.031>.
- [16] Ryttsälä K, Nissilä J, Kokkonen J, Laakso A, Aavikko R, Saarinen K. Digital measurement of positron lifetime. *Appl Surf Sci* 2002;194:260–3. [http://dx.doi.org/10.1016/S0169-4332\(02\)00128-9](http://dx.doi.org/10.1016/S0169-4332(02)00128-9).
- [17] Saito H, Nagashima Y, Kurihara T, Hyodo T. A new positron lifetime spectrometer using a fast digital oscilloscope and BaF2 scintillators. *Nucl Instrum Methods Phys Res A* 2002;487:612–7. [http://dx.doi.org/10.1016/S0168-9002\(01\)02172-6](http://dx.doi.org/10.1016/S0168-9002(01)02172-6).
- [18] Saito H, Hyodo T. Direct measurement of the parapositronium lifetime in  $\alpha$ -SiO<sub>2</sub>. *Phys Rev Lett* 2003;90: 193401. <http://dx.doi.org/10.1103/PhysRevLett.90.193401>.
- [19] Nissilä J, Ryttsälä K, Aavikko R, Laakso A, Saarinen K, Hautojärvi P. Performance analysis of a digital positron lifetime spectrometer. *Nucl Instrum Methods Phys Res A* 2005;538:778–89. <http://dx.doi.org/10.1016/j.nima.2004.08.102>.
- [20] Petschke D. *dpscience/DDRS4PALS: DDRS4PALS (Version 1.08)*. Zenodo. 2019. <http://dx.doi.org/10.5281/zenodo.2540851>.
- [21] Ritt S. Design and performance of the 6 GHz waveform digitizing chip DRS4. In: IEEE Nucl. Sci. Symp. Conf. Rec. IEEE; 2008, p. 1512–5. <http://dx.doi.org/10.1109/NSSMIC.2008.4774700>.
- [22] Paul Scherrer Institut (PSI). DRS4 evaluation board | Paul Scherrer Institut (PSI). 2018. <https://www.psi.ch/drs/evaluation-board>, [Accessed 27 June 2018].
- [23] Ritt S. Documentation DRS4 rev. 0.9. <http://drs.web.psi.ch/datasheets>. [Accessed 15 January 2019].
- [24] Petriska M, Sojak S, Slugeň V. Positron lifetime setup based on DRS4 evaluation board. *J Phys: Conf Ser* 2014;505: 012044. <http://dx.doi.org/10.1088/1742-6596/505/1/012044>.
- [25] Qt Documentation. <https://doc.qt.io/>. [Accessed 22 February 2019].
- [26] Petschke D, Helm R, Staab TEM. Data on pure tin by positron annihilation lifetime spectroscopy (PALS) acquired with a semi-analog/digital setup using DDRS4PALS. *Data Br* 2019;22:16–29. <http://dx.doi.org/10.1016/j.dib.2018.11.121>.
- [27] Petschke D, Staab TEM. *DLTPulseGenerator: A library for the simulation of lifetime spectra based on detector-output pulses*. *SoftwareX* 2018;7:122–8. <http://dx.doi.org/10.1016/j.softx.2018.04.002>.
- [28] Petschke D, Staab TEM. Update (v1.1) to *DLTPulseGenerator: A library for the simulation of lifetime spectra based on detector-output pulses*. *SoftwareX* 2018;7:171–3. <http://dx.doi.org/10.1016/j.softx.2018.05.001>.
- [29] Petschke D, Staab TEM. Update (v1.2) to *DLTPulseGenerator: A library for the simulation of lifetime spectra based on detector-output pulses*. *SoftwareX* 2018;7:259–62. <http://dx.doi.org/10.1016/j.softx.2018.06.003>.
- [30] Petschke D, Staab TEM. Update (v1.3) to *DLTPulseGenerator: A library for the simulation of lifetime spectra based on detector-output pulses*. *SoftwareX* 2019;9:183–6. <http://dx.doi.org/10.1016/j.softx.2019.02.003>.
- [31] Paul Scherrer Institut (PSI). Software download for the DRS4 evaluation board | Paul Scherrer Institut (PSI). 2018. <https://www.psi.ch/drs/software-download>, [Accessed 27 June 2018].
- [32] Bochkannov S, Bystritsky V. *ALGLIB: A cross-platform numerical analysis and data processing library*. 2011. <https://www.alglib.net>.
- [33] Zabinskis S. Sergejus Zabinskis - Fast Median Filtering. [http://www.sergejus.com/engineering\\_tips/median\\_filter.htm](http://www.sergejus.com/engineering_tips/median_filter.htm). [Accessed 22 February 2019].
- [34] Qt Concurrent. <https://doc.qt.io/qt-5.9/qtconcurrent-index.html>. [Accessed 22 February 2019].
- [35] Petschke D. *dpscience/DQuickLTFit: DQuickLTFit v4.0 (Version 4.0)*. Zenodo. 2018. <http://dx.doi.org/10.5281/zenodo.1414142>.
- [36] Bečvář F. Methodology of positron lifetime spectroscopy: Present status and perspectives. *Nucl Instrum Methods Phys Res B* 2007;261:871–4. <http://dx.doi.org/10.1016/j.nimb.2007.03.042>.
- [37] Bečvář F, Čížek J, Procházka I. High-resolution positron lifetime measurement using ultra fast digitizers Acqiris DC211. *Appl Surf Sci* 2008;255:111–4. <http://dx.doi.org/10.1016/j.apsusc.2008.05.184>.

- [38] Barbiellini B, Genoud P, Jarlborg T. Calculation of positron lifetimes in bulk materials. *J Phys: Condens Matter* 1991;3:7631. <http://dx.doi.org/10.1088/0953-8984/3/39/009>.
- [39] Campillo Robles JM, Ogando E, Plazaola F. Positron lifetime calculation for the elements of the periodic table. *J Phys: Condens Matter* 2007;19:176222. <http://dx.doi.org/10.1088/0953-8984/19/17/176222>.
- [40] Istratov AA, Vyvenko OF. Exponential analysis in physical phenomena. *Rev Sci Instrum* 1999;70:1233–57. <http://dx.doi.org/10.1063/1.1149581>.
- [41] Willoughby RA. Solutions of ill-posed problems (A. N. Tikhonov and V. Y. Arsenin). *SIAM Rev* 1979;21:266–7. <http://dx.doi.org/10.1137/1021044>.
- [42] Somieski B, Staab TEM, Krause-Rehberg R. The data treatment influence on the spectra decomposition in positron lifetime spectroscopy Part 1: On the interpretation of multi-component analysis studied by Monte Carlo simulated model spectra. *Nucl Instrum Methods Phys Res A* 1996;381:128–40. [http://dx.doi.org/10.1016/0168-9002\(96\)00584-0](http://dx.doi.org/10.1016/0168-9002(96)00584-0).